Available online at www.sciencedirect.com
SCIENCE DIRECT®
Journal of Crystal Growth 268 (2004) 554–559
JOURNAL OF CRYSTAL GROWTH
www.elsevier.com/locate/jcrysgro

Electronic Structure and Excited-state Properties of Perovskite-like Oxides

P. Ravindran*, R. Vidya, H. Fjellvåg, A. Kjekshus

Department of Chemistry, University of Oslo, P.O. Box 1033 Blindern, N-0315 Oslo, Norway

Abstract

The role of structural distortion, magnetic ordering, and Coulomb-correlation effect on the electronic structure of perovskite-like oxides is analyzed. The density-functional theory (DFT) is originally devised to describe the ground-state properties of materials. However, during recent years it has been seen that the DFT can also be used to study excited state properties succesfully. We have recently calculated the electronic structure and linear optical properties for the series $LaXO_3$ (X = Sc–Cu) and found that the gradient-corrected DFT describes correctly the insulating behavior of the ionic insulator $LaScO_3$ and the charge-transfer insulators $LaCrO_3$, $LaFeO_3$, and $LaMnO_3$ although the band gaps are systematically underestimated. For example, the good agreement between experimental and theoretical reflectivity spectra for $LaCrO_3$ clearly demonstrates that accurate full-potential DFT calculations not only describe the occupied and unoccupied states of the bands well, but also reproduce their characters. We have also calculated XPS, XANES, and magneto-optical spectra for perovskite-like oxides. For Mott–Hubbard insulators such as $LaTiO_3$ and $LaVO_3$ the DFT failed to predict insulating behavior and here the LDA + U method is applied to describe the electronic structure correctly.

PACS: 70; 78.20.Ls; 78.20.Ci; 74.25.Gz

Keywords: B1. Perovskites; B2. Magnetic materials; B2. Semiconducting ternary compounds

1. Introduction

The simultaneous presence of strong electron–electron interactions within the transition-metal-3d manifold and a sizable hopping interaction between transition-metal-3d (T = Ti–Cu) and O-2p states are primarily responsible for the wide range of properties exhibited by transition-metal oxides. Often the presence of a strong intra-atomic Coulomb interaction makes a single-particle description of such systems inadequate. Due to this deficiency, the density-functional calculations often fail to predict the insulating behavior of transition-metal oxides. To correct this deficiency of the local spin-density approximation (LSDA) and to provide the right insulating properties of the perovskites, LSDA + U theory [1,2] is applied, where U is the intra-site Coulomb repulsion. The

*Corresponding author. Tel.: +47-22-855-606; fax: +47-22-855-441.

E-mail addresses: ponniah.ravindran@kjemi.uio.no, ravindran.ponniah@kjemi.uio.no (P. Ravindran).

URL: http://folk.uio.no/ravi.

0022-0248/$ - see front matter © 2004 Elsevier B.V. All rights reserved.
doi:10.1016/j.jcrysgro.2004.04.090

calculations for $LaTO_3$ by Solovyev et al. [3] showed that the correlation correction was significant for Ti, V, and Co, but less important for Mn. However, in this study the calculated intensity of the optical conductivity were found to be much smaller than the experimental values in the whole energy range. Hu et al. [4] reported that to obtain the correct experimental ground state for $LaMnO_3$, it is necessary to take JT distortion, electron–electron correlation, and AF ordering simultaneously into consideration. Density-functional calculations also show strong couplings between lattice distortions, magnetic order, and electronic properties of $LaTO_3$. Owing to the presence of magnetic ordering, relativistic effects such as spin–orbit coupling (not included in most of the earlier studies) may be of significance in this material. Moreover, it is seen that instead of using the uniform electron-gas limit for exchange and correlations (corresponding to LSDA) one can improve the outcome by including the inhomogeneity effects through the generalized-gradient approximation (GGA) [5]. To overcome the above mentioned deficiencies we have used a generalized-gradient-corrected, relativistic full-potential method with the experimentally established $GdFeO_3$-type distorted perovskite structure as the input in the present calculation. From the results obtained from these calculations we have also studied excited-state properties of these materials.

2. Computational details

We used the ab initio GGA [6] to obtain accurate exchange and correlation energies. The experimentally observed structural parameters are used in the calculations and no attempt has been made to optimize it. In order to understand the role of structural distortion on electronic structure and magnetic properties of $LaMnO_3$ we have also considered the ideal cubic perovskite structure with the equilibrium volume of the orthorhombic structure. The relativistic full-potential linear muffin-tin orbital (FP-LMTO) [7] method has been used for the total energy and DOS calculations. For the LSDA + U calculation we have used the projected augmented wave (PAW) implementation of the Vienna ab initio simulation package (VASP) [8]. The calculations were performed for "nonmagnetic" (P), ferromagnetic (F), antiferromagnetic A–AF, C–AF, and G–AF states, and the density of states (DOS) are calculated for the ground state. The **k**-space integration was performed using the special point method with 284 **k** points in the irreducible part of the first Brillouin zone for the orthorhombic structure and the same density of **k** points were used for the cubic structure. Using the self-consistent potentials obtained from our calculations, the excited state properties are derived and DOS curves were calculated using the linear tetrahedron technique.

3. Results and discussion

The calculated total DOS curves for $LaScO_3$, $LaCrO_3$, and $LaFeO_3$ are given in Fig. 1. All the

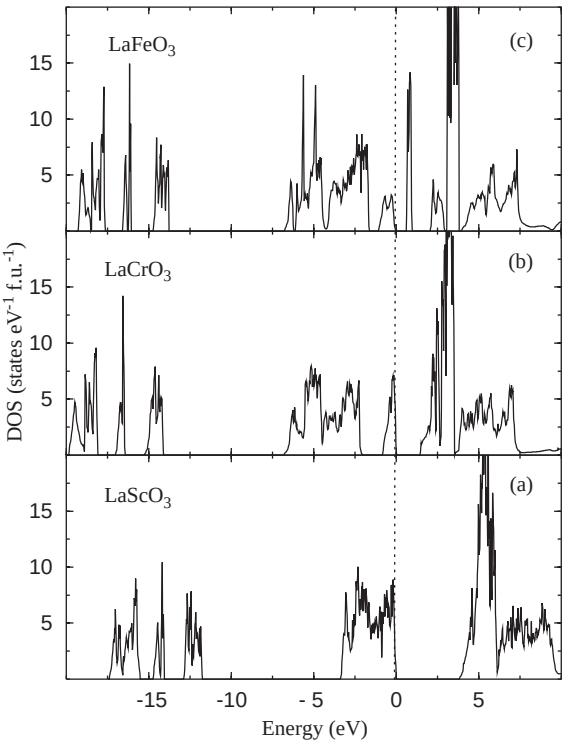

Fig. 1. Calculated total density of states for (a) $LaScO_3$, (b) $LaCrO_3$, and (c) $LaFeO_3$ in their ground state. The Fermi level is set to zero and marked by the vertical line.

three compounds are stabilized in the orthorhombic $GdFeO_3$-type structure, where $LaScO_3$ is in the "nonmagnetic" phase and $LaCrO_3$ and $LaFeO_3$ are in the *G*–AF phase in the ground state. In all the three compounds the FP-LMTO calculations successfully reproduced the experimentally observed insulating behavior. We have obtained a band gap of 3.98, 1.45, and 0.67 eV for $LaScO_3$, $LaCrO_3$, and $LaFeO_3$, respectively. However, optical measurements [9] gave a optical gap of 6, 3.5, and 2 eV, respectively. It should be noted that we were able to reproduce the decreasing trend in gap value from $LaScO_3$ to $LaFeO_3$, but the calculated values are smaller than the experimental values. The calculated band gap is here identified as the difference between the highest occupied and the lowest unoccupied Kohn–Sham eigenvalues, the so-called Kohn–Sham gap. The real band gap, however, is the smallest difference between the energy required to remove an electron from the valence band of the insulating *N*-particle ground state to infinity and the energy obtained by adding an electron to the conduction band of the insulating *N*-particle ground state. This real band gap can be written as a sum of the Kohn–Sham gap and a part originating from the discontinuity in the exchange-correlation potential at the integer particle number *N* [10]. Because of the difficulties with the discontinuity, there are no standard methods for calculating (correctly) the size of band gaps, although recent work based on the GW approximation seems promising in this regard [11]. Though the calculated band gap is underestimated, the reflectivity spectra for $LaCrO_3$ obtained from Kramers Kronig transformed $\varepsilon_2(\omega)$ spectra by summing transitions from occupied to unoccupied states (with fixed **k** vector) over the Brillouin zone (weighted with the appropriate matrix element [12]) is found to be in good agreement with the experimental spectra [9] (see Fig. 4a). This indicates that the present type of calculations place the occupied and unoccupied states accurately up to higher energies.

The importance of spin and lattice degrees of freedom for the metal–insulator transition in $LaMnO_3$ is studied extensively [13]. Popovic and Satpathy [14] showed how the cooperative JT coupling between the individual MnO_6 centers in the crystal leads to simultaneous ordering of the distorted octahedra and the electron orbitals. It is now accepted that orbital ordering (OO) and magnetic ordering (MO) are closely correlated and that the anisotropy in the magnetic coupling originates from OO [15]. $LaMnO_3$ is stabilized in the orthorhombic $GdFeO_3$-type structure [16,17] which can be viewed as a highly distorted cubic perovskite structure with a quadrupled unit cell ($a_p\sqrt{2}$, $a_p\sqrt{2}$, $2a_p$ where a_p is the lattice parameter of the cubic perovskite structure. Basically, two different types of distortions are included in this structure. One is a tilting of the MnO_6 octahedra around the cubic [1 1 0] axis so that the Mn–O–Mn angle changes from 180° to ~160° which is attributed to the relative sizes of the components, say, expressed in terms of the tolerance factor

$$t_p = \frac{R_{La} + R_O}{\sqrt{2}(R_{Mn} + R_O)},$$

where R_{La}, R_{Mn}, and R_O are the radii for La, Mn, and O, respectively; giving $t_p = 0.947$ for $LaMnO_3$. The rotation of the MnO_6 octahedra facilitates a more efficient space filling. The second type of crystal distortion in $LaMnO_3$ is the deformation of the MnO_6 octahedra caused by the JT effect, viz. originating from orbital degeneracy. This may be looked upon as a cooperative shifting of the oxygens within the *ab* plane away from one of its two nearest neighboring Mn atoms toward the others, thus creating long and short Mn–O bond lengths (modified from 1.97 Å for cubic case to 1.91, 1.96, and 2.18 Å for the orthorhombic variant) perpendicularly arranged with respect to the Mn atoms. We have made calculations both for the orthorhombic (*Pnma*) and the ideal cubic perovskite variants. For the calculations of the undistorted cubic variant we have used the experimental equilibrium volume for the orthorhombic structure.

Our total energy studies on $LaMnO_3$ in *A*–, *C*–, *G*–AF, F, and "nonmagnetic" states show that the ground state is semiconducting *A*–AF in the orthorhombic phase and half-metallic F in the hypothetical cubic phase [18]. In order to understand the role of the crystal structure on the electronic structure of $LaMnO_3$, the calculated total DOS for $LaMnO_3$ in the cubic *A*–AF and

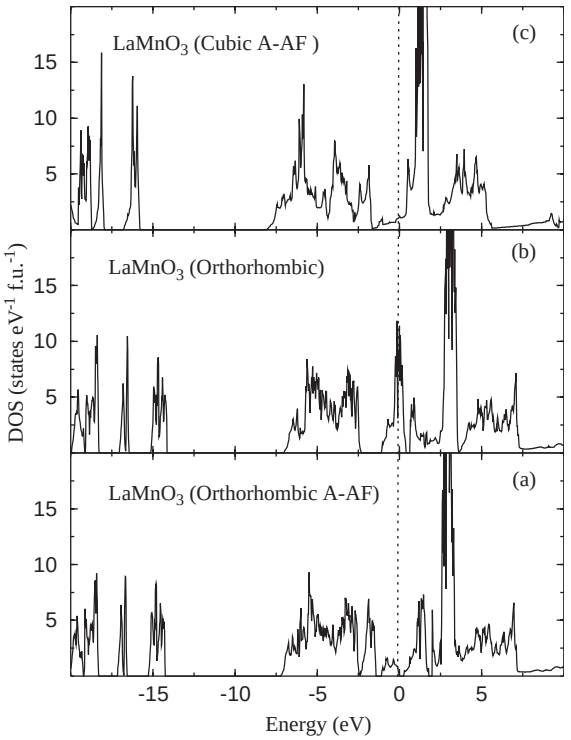

Fig. 2. Calculated total density of states for $LaMnO_3$ in (a) the orthorhombic A–AF, (b) orthorhombic "nonmagnetic", and (c) cubic A–AF phases. The Fermi level is set to zero and marked by the vertical dashed line.

orthorhombic A–AF states is given in Fig. 2a,c, respectively. The orthorhombic A–AF state is found to be semiconducting with a 0.278 eV gap between the e_g levels consistent with the observed insulating behavior in this material. Using the LAPW method, Pickett and Singh [19] obtained a gap of 0.12 eV for the distorted $LaMnO_3$ when they include the JT effect and A–AF ordering. In contrast, for the hypothetical cubic perovskite structure, even when A–AF ordering is included in the calculations, we found metallic behavior as seen from the finite DOS at the Fermi level (see Fig. 2b). This indicates that it is important to include structural distortion into the calculations to correctly predict insulating behavior in transition-metal oxides. To understand the role of magnetic ordering on the electronic structure, the calculated total DOS for $LaMnO_3$ in the "nonmagnetic" orthorhombic phase is given in Fig. 2b. Observation of metallic behavior in the "nonmagnetic" case clearly shows that it is important to include proper magnetic ordering in addition to the structural distortions into the calculation to predict correctly the insulating behavior in transition-metal oxides.

The Mott–Hubbard-type $LaVO_3$ has monoclinic structure at low temperature and C-type AF ordering with an observed optical gap of $\sim$1.1 eV below 140 K [20,21,9]. Our total energy studies on $LaVO_3$ in the A–, C–, G–AF, F, and "nonmagnetic" configurations show that the C–AF phase has the lowest energy consistent with the experiments. Our calculated magnetic moment at the vanadium site is 1.51 μ_B which is in good agreement with the experimental value of 1.3 μ_B obtained from a neutron scattering study [20]. Though the magnetic property of this material is correctly predicted, the usual generalized-gradient-corrected relativistic full-potential calculation which takes into account structural distortion and proper magnetic ordering failed to predict the experimentally found insulating behavior. So, our calculated total DOS given in Fig. 3b show metallic behavior with a DOS value at E_F of 2.93 states $eV^{-1}f u^{-1}$. This failure is owing to a strong Coulomb correlation effect present in this

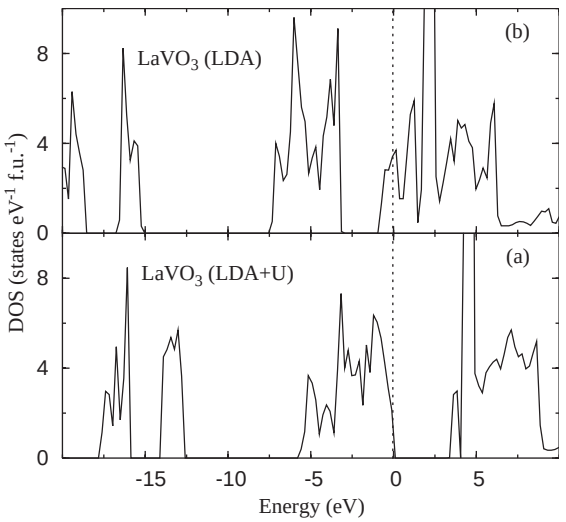

Fig. 3. Calculated spin projected total density of states for $LaVO_3$ obtained from (a) LDA and (b) LDA + U calculation in the C–AF monoclinic phase. The Fermi level is set to zero and marked by the vertical dashed line.

material. Our constrained density-functional calculations yielded a Coulomb correlation energy (U) of 8.1 eV in $LaVO_3$. Using this U value we have made LDA + U calculation for $LaVO_3$ in the monoclinic C–AF phase and the total DOS thus obtained (see Fig. 3a) clearly show insulating behavior consistent with optical measurements. So, it is important to include Coulomb correlation effects into the calculation for strongly correlated materials to correctly predict their electronic structure.

We have also calculated XPS, BIS, and UPS spectra for the considered transition-metal oxides and show as an example the calculated XPS spectrum of A–AF $LaMnO_3$ in Fig. 4b along with the experimental spectrum [22]. The XPS spectrum gives information about the valence band. The experimental XPS data show three peak features between −7 and −3 eV. As can be seen from Fig. 4, these three peaks are well reproduced in the calculated profile. From Fig. 4b it is clear that the XPS intensity in the energy range −3.5 eV to E_F mainly originates from Mn-d states. The O-p electrons contribute to the PES intensity in the energy range −7–3.5 eV. Below −4 eV both La and Mn atoms contribute equally to the PES intensity. The calculated Mn K-edge XANES spectrum of $LaMnO_3$ is shown in Fig. 4c along with experimental spectra for the A–AF phase [23–25]. Because of the angular momentum selection rule Mn-4p states contribute to the Mn K-edge spectrum. Mn K-edge spectrum is found to be in very good agreement with that of Subias et al. [23] in the whole energy range considered here. The good agreement between experimental and calculated XANES spectra further emphasizes the relatively little significance of correlation effects in $LaMnO_3$ and also shows that the gradient-corrected full-potential approach is able to predict even the unoccupied states quite correctly.

The investigation of compounds with high magneto-optical activity is of great importance both for development of high density magneto-optical (MO) disks and for achieving a deeper understanding of the electronic structure and magnetic properties of solids. We have calculated the MO properties such as Kerr and Faraday spectra for a series of F materials. The calculated

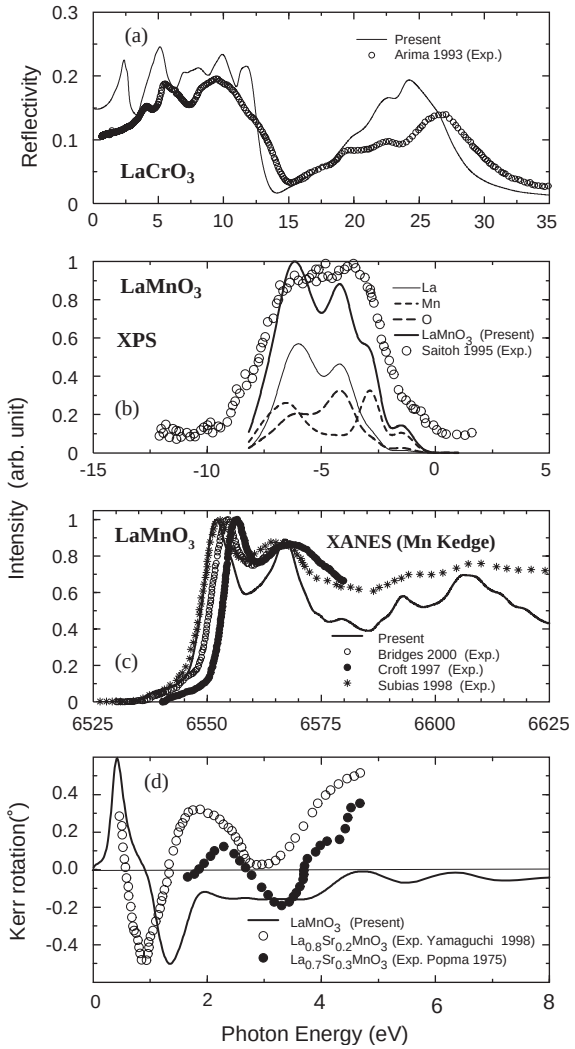

Fig. 4. (a) Calculated reflectivity spectra for $LaCrO_3$ in the G–AF structure, (b) XPS and (c) XANES spectra for $LaMnO_3$ in the A–AF phase and (d) Kerr rotation spectrum for $LaMnO_3$ in the F phase. Experimental data are quoted from Refs. [9,22–27].

Kerr-rotation spectrum for F-state $LaMnO_3$ is shown in Fig. 4d along with experimental spectra obtained for hole-doped materials in the same state [26,27]. MO effects are proportional to the product of the SO-coupling strength and the net electron-spin polarization. This makes MO effects sensitive to the magnetic electrons, i.e., to the 3d electrons of Mn in $LaMnO_3$. Even though the experimental MO spectrum for $La_{0.8}Sr_{0.2}MnO_3$

was measured [26] at 300 K with a magnetic field of 2.2 kOe, our calculated Kerr rotation spectrum is comparable in the lower-energy region (Fig. 4d). The discrepancy between the experimental and theoretical Kerr spectra in the higher-energy region may be explained as a temperature and/or hole doping effect.

In summary, the importance of magnetic ordering, structural distortions, and correlation effect on the electronic structure of perovskite-like transition-metal oxides is analyzed. The advantage of doing theoretical calculation of excited state properties is that from these studies we can not only predict the exited state properties but also identify the microscopic origins for features in the experimentally observed spectra.

Acknowledgements

This work has received financial support from the Norwegian Research Council.

References

[1] V.I. Anisimov, J. Zaanen, O.K. Andersen, Phys. Rev. B 44 (1991) 943.
[2] I.V. Solovyev, P.H. Dederichs, V.I. Anisimov, Phys. Rev. B 50 (1994) 16861.
[3] I.V. Solovyev, N. Hamada, K. Terakura, Phys. Rev. B 53 (1996) 7158.
[4] W.Y. Hu, M.C. Qian, Q.Q. Zheng, H.Q. Lin, H.K. Wang, Phys. Rev. B 61 (2000) 1223.
[5] H. Sawada, Y. Morikawa, K. Tarakura, N. Hamada, Phys. Rev. B 56 (1997) 12154.
[6] J.P. Perdew, in: P. Ziesche, H. Eschrig (Eds.), Electronic Structure of Solids, Akademie Verlag, Berlin, 1991, p.11;
J.P. Perew, K. Burke, Y. Wang, Phys. Rev. B 54 (1996) 16533;
J.P. Perdew, S. Burke, M. Ernzerhof, Phys. Rev. Lett. 77 (1996) 3865.
[7] J.M. Wills, O. Eriksson, M. Alouani, D.L. Price, in: H. Dreysse (Ed.), Electronic Structure and Physical Properties of Materials, Springer, Berlin, 2000, p. 148.
[8] G. Kresse, J. Hafner, Phys. Rev. B 47 (1993) 558;
G. Kresse, J. Furthmuller, Comput. Mater. Sci. 6 (1996) 15;
P.E. Blöchl, Phys. Rev. B 50 (1994) 17953;
G. Kresse, D. Joubert, Phys. Rev. B 59 (1999) 1758.
[9] T. Arima, Y. Tokura, J.B. Torrance, Phys. Rev. B 48 (1993) 17006.
[10] R.M. Dreizler, E.K.U. Gross, Density Functional Theory: an Approach to the Quantum Many-Body Problem, Springer, Berlin, 1990.
[11] F. Bechstedt, R. Del Sole, Phys. Rev. B 38 (1988) 7710.
[12] P. Ravindran, A. Delin, B. Johansson, O. Eriksson, J.M. Wills, Phy. Rev. B 59 (1999) 1776.
[13] O.N. Mryasov, R.F. Sabiryanov, A.J. Freeman, S.S. Jaswal, Phys. Rev. B 56 (1997) 7255.
[14] Z. Popovic, S. Satpathy, Phys. Rev. Lett. 84 (2000) 1603.
[15] I.V. Solovyev, K. Terakura, J. Korean, Phys. Soc. 33 (1998) 375.
[16] G. Matsumoto, J. Phys. Soc. Japan. 29 (1970) 606.
[17] J.B.A.A. Elemans, B.V. Laar, K.R.V.D. Veen, B.O. Looptra, J. Solid State Chem. 3 (1971) 238.
[18] P. Ravindran, A. Kjekshus, H. Fjellvåg, A. Delin, O. Eriksson, Phys. Rev. B 65 (2002) 064445.
[19] W.E. Pickett, D.J. Singh, Phys. Rev. B 53 (1996) 1146.
[20] V.G. Zubkov, G.V. Bazuev, V.A. Perelyaev, G.P. Shveikin, Sov. Phys. Solid State 15 (1973) 1079.
[21] P. Bordet, C. Chaillout, M. Marezio, Q. Huang, A. Santoro, S. Cheong, H. Takagi, C. Oglesby, B. Batlogg, J. Solid State Chem. 106 (1993) 253.
[22] T. Saitoh, A.E. Bocquet, T. Mizokawa, H. Namatame, A. Fujimori, M. Abbate, Y. Takeda, M. Takano, Phys. Rev. B 51 (1995) 13942.
[23] G. Subias, J. Garcia, J. Blasco, M.G. Proietti, Phys. Rev. B 58 (1998) 9287.
[24] F. Bridges, C.H. Booth, G.H. Kwei, J.J. Neumeier, G.A. Sawatzky, Phys. Rev. B 61 (2000) R9237.
[25] M. Croft, D. Sills, M. Greenblatt, C. Lee, S.-W. Cheong, K.V. Ramanujachary, D. Tran, Phys. Rev. B 55 (1997) 8726.
[26] S. Yamaguchi, Y. Okimoto, K. Ishibashi, Y. Tokura, Phys. Rev. B 58 (1998) 6862.
[27] T.J.A. Popma, M.G.J. Kamminga, Solid State Commun. 17 (1975) 1073.